

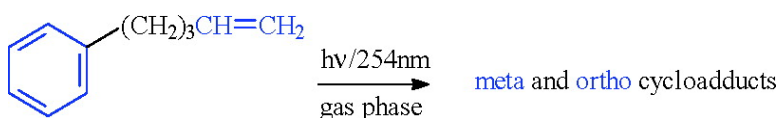
Article

Photochemistry of 5-Phenyl-1-pentene in the Gas Phase

Chang-Dar D. Ho, and Harry Morrison

J. Am. Chem. Soc., **2005**, 127 (7), 2114-2124 • DOI: 10.1021/ja044504z • Publication Date (Web): 01 February 2005

Downloaded from <http://pubs.acs.org> on March 24, 2009



More About This Article

Additional resources and features associated with this article are available within the HTML version:

- Supporting Information
- Links to the 2 articles that cite this article, as of the time of this article download
- Access to high resolution figures
- Links to articles and content related to this article
- Copyright permission to reproduce figures and/or text from this article

[View the Full Text HTML](#)



ACS Publications
High quality. High impact.

Photochemistry of 5-Phenyl-1-pentene in the Gas Phase

Chang-Dar D. Ho and Harry Morrison*

*Contribution from the Department of Chemistry, Purdue University,
West Lafayette, Indiana 47907*

Received September 10, 2004; E-mail: hmorrison@purdue.edu

Abstract: The photochemistry of the title compound has been studied in the gas phase using 254-nm irradiation. In addition to meta cycloadducts analogous to those observed in solution, population of S_1^{vib} in the gas phase gives several products, the relative amounts of which depend on quencher gas pressure but not on excitation wavelength. For example, in the absence of butane, the major photoproduct is compound **5**. This product is formed by a [1,5] hydrogen shift in the primary photoproduct, compound **4**. Compound **4** is an intramolecular meta cycloadduct that is generated in the gas phase with sufficient excess vibrational energy to undergo rearrangement unless quencher gas is present. Likewise, there is evidence that two other meta cycloadducts (**2** and **3**) are also formed with appreciable vibrational energy in the absence of a quencher gas. A unique intramolecular ortho cycloadduct is also formed from **1** but only within a narrow range of quencher gas pressures. This is a two-photon product, with the initial cycloadduct (**11**) ring opening to a cyclooctatriene (**12**) that photochemically closes to **6**. The pressure dependence of this ortho cycloaddition may be due to a requirement for vibrational deactivation of **11** (Scheme 5) or a precursor species (Scheme 6). The overall chemistry is outlined in Scheme 7.

Introduction

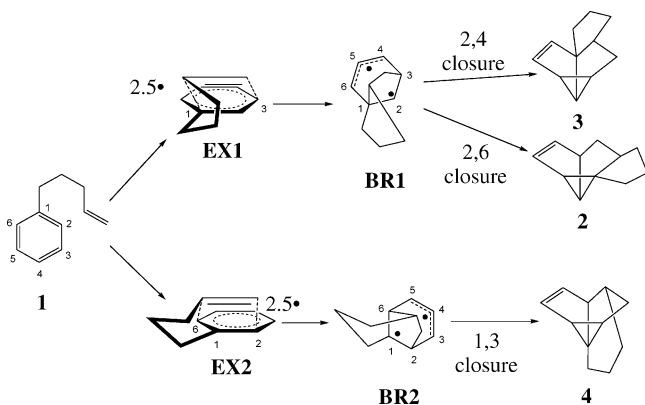
The study of the photochemistry of nonconjugated arylalkenes has been a source of interest for several decades. A particularly fascinating early observation was that a double bond three carbons removed from a benzene ring is highly successful in trapping the phenyl S_1 excited state.¹ On the basis of the reduction in lifetime of the phenyl S_1 state from 35 ns (toluene) to 2.5 ns, these workers proposed that the alkene traps the phenyl S_1 excited state to form an exciplex. They suggested that the exciplex then converts to the intramolecular meta(1,3)-cycloadducts that were observed as the primary products.¹ The intramolecular meta photocycloaddition reaction was subsequently extended, analyzed, and utilized by numerous workers.² Gilbert and co-workers studied the effect of aryl and alkene substituents and proposed a more detailed mechanism³ that was analogous to proposals to rationalize the intermolecular photoreactions of

substituted benzenoid compounds with ethenes.^{4–7} The proposed mechanism involves the formation of a pair of exciplexes (**EX1** and **EX2**) followed by the generation of a pair of diradical intermediates (**BR1** and **BR2**). Using 5-phenyl-1-pentene (**1**) as an example (Scheme 1), the 2,4 closure of **BR1** forms meta cycloadduct **3** while the formation of a 2,6 bond in this biradical gives **2**. Likewise, there are two modes of closure for **BR2**. One, 1,3 closure, leads to adduct **4**, but closure of the 1,5 bond in **BR2** would give a severely strained product that is rarely observed.

Though the diradical mechanism explained products formed in the parent system, it did not rationalize the difference in regioselectivity seen in the presence of electronegative and electropositive substituents nor the effect of solvent polarity. Through the efforts of numerous workers, the mechanism was therefore extended to involve partially zwitterionic intermediates instead of full diradicals.^{2b,8} However, the regioselectivity of meta cycloadduct formation is basically predetermined by the conformations of the exciplexes,^{2b,3} an aspect that was extensively studied by Wender's group.^{2a,2c} With the proper design of substituents on the benzene and alkene moieties, photoinduced

- (1) (a) Morrison, H.; Ferree, W. I., Jr. *J. Chem. Soc., Chem. Commun.* **1969**, 268–269. (b) Ferree, W. I., Jr.; Grutzner, J. B.; Morrison, H. *J. Am. Chem. Soc.* **1971**, *93*, 5502–5512.
- (2) For reviews, see: (a) Wender, P. A.; Siggel, L.; Nuss, J. M. In *Comprehensive Organic Synthesis. Selectivity, Strategy and Efficiency in Modern Organic Chemistry*; Trost, B. M., Fleming, I., Paquette, L. A. Eds.; Pergamon Press: Oxford, 1991; Vol. 5, pp 645–673. (b) Cornélisse, J. *Chem. Rev.* **1993**, *93*, 615–669. (c) Wender, P. A.; Dore, T. M. *CRC Handbook of Organic Photochemistry and Photobiology*; Horspool, W. M., Song, P. S., Eds; CRC Press: Boca Raton, FL, 1995; pp 280–290. (d) Mizuno, K.; Maeda, H.; Sugimoto, A.; Chiyonobu, K. In *Molecular and Supramolecular Photochemistry. Understanding and Manipulating Excited-State Processes*; Ramamurthy, V., Schanze, K. S., Eds.; Marcel Dekker: New York, 2001; Vol. 8, pp 127–241. (e) Gilbert, A. *CRC Handbook of Organic Photochemistry and Photobiology*, 2nd ed.; Horspool, W. M., Lenci, F., Eds; CRC Press: Boca Raton, FL, 2004; pp 41–1–41–11. (f) Hoffmann, N. *Synthesis* **2004**, 481–495.
- (3) (a) Gilbert, A.; Taylor, G. N. *J. Chem. Soc., Perkin Trans. 1* **1980**, 1761–1768. (b) Ellis-Davies, G. C. R.; Gilbert, A.; Heath, P.; Lane, J. C.; Warrington, J. V.; Westover, D. L. *J. Chem. Soc., Perkin Trans. 2* **1984**, 1833–1841.

- (4) (a) Cornélisse, J.; Merrit, V. Y.; Srinivasan, R. *J. Am. Chem. Soc.* **1973**, *95*, 6197–6203. (b) Merrit, V. Y.; Cornélisse, J.; Srinivasan, R. *J. Am. Chem. Soc.* **1973**, *95*, 8250–8255. (c) Srinivasan, R.; Ors, J. A. *Chem. Phys. Lett.* **1976**, *42*, 506–508. (d) Ors, J. A.; Srinivasan, R. *J. Org. Chem.* **1977**, *42*, 1321–1327.
- (5) Sheridan, R. S. *Tetrahedron Lett.* **1982**, *23*, 267–270.
- (6) Bryce-Smith, D.; Fenton, G. A.; Gilbert, A. *Tetrahedron Lett.* **1982**, *23*, 2697–2700.
- (7) Mattay, J.; Runsink, J.; Leismann, H.; Scharf, H. D. *Tetrahedron Lett.* **1982**, *23*, 4919–4922.
- (8) Cornélisse, J.; de Haan, R. *Molecular and Supramolecular Photochemistry, Vol. 8*; Ramamurthy, V., Schanze, K. S., Eds.; Marcel Dekker: New York, 2001; pp 1–126.

Scheme 1. Biradical Mechanism for Intramolecular Meta Cycloaddition of 5-Phenyl-1-pentene (**1**) in Solution

intramolecular meta cycloaddition has become a powerful tool in the synthesis of polycyclic natural products.^{2f}

Ortho cycloaddition often competes with meta cycloaddition in intermolecular photocycloaddition reactions involving benzene derivatives and alkenes.^{2e,8} Through studies of the effect of the ionization and redox potentials of various benzenes and alkenes on the photochemistry, it has been demonstrated that the difference in these potentials for the reaction pair plays an important role in the competition between meta and ortho cycloaddition.^{2b,8} Using the Rehm–Weller equation to estimate the degree of charge transfer in the exciplexes, it was noted that cycloaddition involving reactant pairs having little charge transfer generally leads to meta cycloadducts, while those reactions in which charge transfer is energetically favored are dominated by ortho cycloaddition.^{9,10} This rule is followed even more strictly in intramolecular cycloaddition. The photocycloaddition between a simple alkyl substituted benzene and an internal alkene always leads to meta cycloadducts.^{2d,8}

Our interest in examining the photochemistry of 5-phenyl-1-pentene (**1**) in the gas phase stemmed from the fact that the alkene group in **1** is capable of intercepting the aryl singlet excited state with a rate constant of $0.37 \times 10^9 \text{ s}^{-1}$ in solution.¹ Photochemistry in the gas phase is useful for probing reactions that occur in upper electronic excited states (i.e., S_2) or vibrationally excited states (S_1^{vib}), and we have made some novel observations upon applying this technique to several aromatic hydrocarbons.¹¹ For example, the gas-phase photochemistry of 3-methyl-1,2-dihydronaphthalene leads to several new products unique to the gas phase that derive from the “hot” vibronic excited states of S_2 or S_1 .¹² In benzene itself, upper vibronic states of S_1 are involved in the so-called “channel-three” radiationless decay that occurs when benzene is excited with $\sim 3000 \text{ cm}^{-1}$ of excess vibrational energy above the S_1 origin.¹³ We thus thought it of interest to see if the rapid interaction of an alkene appended to a benzene ring could provide information

Table 1. Quantum Yields for the Photolysis of **1** in Cyclohexane as a Function of Excitation Wavelength

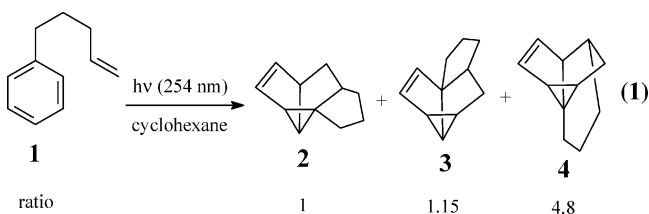
λ_{ex} (nm)	$\Phi_{\text{cyc}} (\times 10^{-2})$	$\Phi_2 (\times 10^{-2})$	$\Phi_3 (\times 10^{-2})$	$\Phi_4 (\times 10^{-2})$
255	13.0 ± 1.0	1.7 ± 0.2	2.2 ± 0.4	9.1 ± 0.4
266	11.0 ± 0.8	1.4 ± 0.2	1.9 ± 0.3	7.7 ± 0.3

about the benzene S_1^{vib} states or about transients derived from these states. We chose the simplest model, compound **1**, and have, in fact, observed photochemistry not seen in solution. Time-course studies, and the effects of quencher gases and excitation wavelengths, have been used to understand the origin of this new gas-phase photochemistry.

Results

Preparation of 5-Phenyl-1-pentene (1). 5-Phenyl-1-pentene was prepared by the Grignard coupling of 1-bromo-2-phenylethane with allylmagnesium bromide. Distillation, silica gel flash chromatography, and finally preparative GLC provided samples of $\geq 99\%$ purity. The compound has been prepared previously and its ^1H NMR spectrum was consistent with that in the literature.¹⁴ The UV absorption spectrum for **1** in cyclohexane (Supporting Information) shows structured absorption between 230 and 280 nm. This corresponds to the first electronic transition ($S_0 \rightarrow S_1$), and the λ_{max} at 260 nm (ϵ , $215 \text{ M}^{-1}\text{cm}^{-1}$) is unexceptional. The spectrum is quite similar to the absorption spectrum reported for *cis*-6-phenyl-2-hexene in hexane.¹ The UV absorption spectrum for toluene in the gas phase also shows a λ_{max} at 260 nm with $\epsilon = 103 \text{ M}^{-1}\text{cm}^{-1}$.¹⁵

Solution Phase Photolysis of 1. As noted in the Introduction, the photolysis of **1** in solution has been extensively studied.³ We reproduced those results and found that irradiation with 254 nm light gave the three products (**2**, **3**, **4**) previously reported, with a comparable product ratio (eq 1).



The quantum yields for loss of **1** were determined by excitation into the long- and short-wavelength portions of the first electronic absorption band using lasers. The values (F_{cyc}) we determined at 266 nm (0.11) and at 255 nm (0.13) are comparable to that (0.15) reported in Gilbert’s work³ using 254-nm low-pressure mercury arc light. GLC analysis using an internal standard confirmed that the observable products account for 100% of the starting material lost. The complete set of data is listed in Table 1.¹⁶

Gas Phase Photolysis of 1 under Flowing Conditions. Compound **1** was photolyzed in the gas phase under low-pressure, “flowing conditions” (see Experimental) at 254 nm. The photolysis produced a new compound, **5**, and traces of compounds **2** and **3**. Compound **5** was shown by mass spectral analysis to be isomeric with **1**, and its ^1H NMR spectrum was identical with that reported^{3a} for the structure shown in eq 2.

(9) (a) Mattay, J. *Tetrahedron* **1985**, *41*, 2393–2404. (b) Mattay, J. *Tetrahedron* **1985**, *41*, 2405–2417.

(10) Müller, F.; Mattay, J. *Chem. Rev.* **1993**, *93*, 99–117.

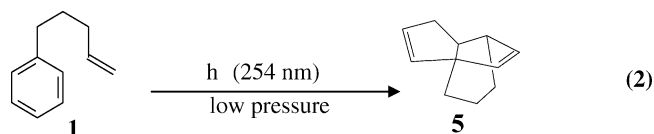
(11) Waugh, T.; Morrison, H. *J. Am. Chem. Soc.* **1999**, *123*, 3083–3092, and references therein.

(12) Duguid, R. J.; Morrison, H. *J. Am. Chem. Soc.* **1991**, *113*, 1271–1281.

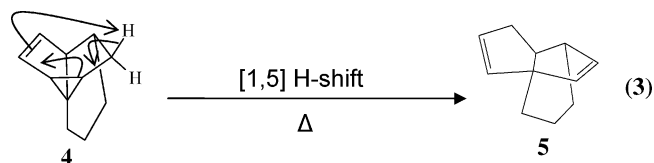
(13) (a) Callomon, J. H.; Parkin, J. E. *Chem. Phys. Lett.* **1972**, *13*, 125–131. (b) Riedle, E.; Weber, Th.; Schubert, U.; Neusser, H. J.; Schlag, W. *J. Chem. Phys.* **1990**, *93*, 967–978. (c) Palmer, I. J.; Ragazos, I. N.; Bernardi, F.; Olivucci, M.; Robb, M. *J. Am. Chem. Soc.* **1993**, *115*, 673–682. (d) Chachisvilis, M.; Zewail, A. H. *J. Phys. Chem. A* **1999**, *103*, 7408–7418.

(14) Gamage, S. A.; Smith, R. A. *J. Tetrahedron* **1990**, *46*, 2111–2128.

(15) Hipper, H.; Troe, J.; Wendelken, H. *J. Chem. Phys.* **1983**, *78*, 5351–5357.



Compound **5** is formed by a [1,5] H-shift in **4** which earlier workers had observed during GLC analysis (see eq 3).^{3a} We too observed this rearrangement when the GLC column oven temperature was >150 °C or the injection port temperature was >220 °C.

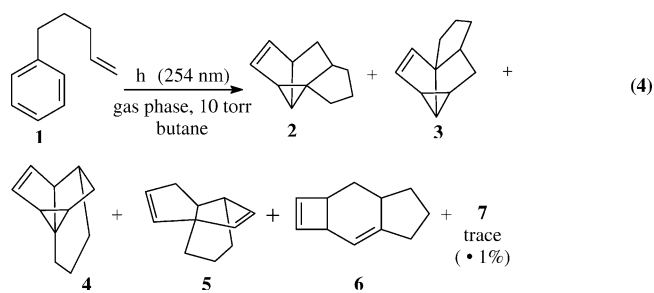


Effect of Butane on the Gas-Phase Photochemistry of **1**.

Compound **1** was photolyzed in the presence of varying pressures of butane gas under “static” (see Experimental) conditions. The loss of starting material is plotted in Figure 1, and the formation of compounds **2–5** are plotted in Figures 2 and 3. All area percentages represent the fraction of the total integrated area for products and starting material since mass balance analyses in several static photolysis experiments using an internal standard indicated that $>98\%$ of the disappearing **1** was converted to these products.

Figure 3 includes a new product, **6**, that has not been discussed. This product is not observed in the absence of butane and is seen primarily at medium pressures (ca. 10 Torr) of the quencher gas (see Figure 3). It is also formed in trace amounts ($<0.5\%$) in solution upon prolonged photolysis (>60 min). In fact, compound **6** was eventually isolated from a series of preparative, prolonged, solution-phase photolyses of **1**. Its structure assignment was based on an analysis of its ^1H and ^{13}C NMR, UV–vis, and mass spectra. The assignment of structure is discussed in detail in the Discussion section.

In addition to the major products described above, a trace ($\leq 1\%$) amount of an unidentified material (**7**) was also detected under medium butane pressure conditions. This compound was not seen in the absence of butane nor in the solution-phase photolysis. It was not isolated because of its low yield, but a GLC/mass spectrum indicated that it is an isomer of **1** ($m/e = 146$). The gas-phase photolysis of **1** in the presence of ca. 10 Torr butane is summarized in eq 4.



(16) There is clearly no wavelength effect on this photochemistry in solution. This contradicts an earlier report of a wavelength effect in the photochemistry of 6-phenyl-2-hexene.¹ That work was done with a grating monochromator with limited light intensities.

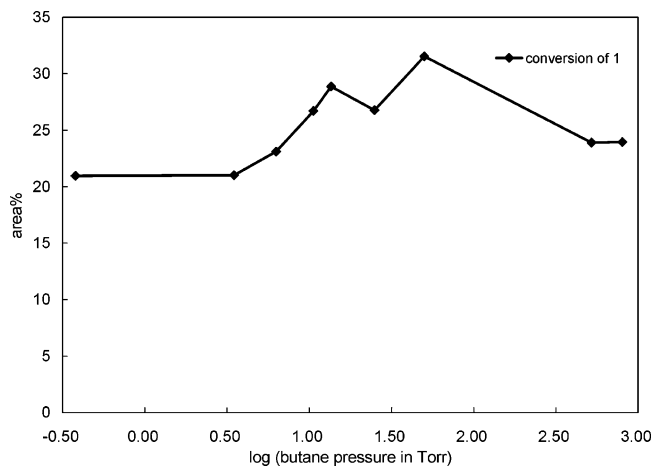


Figure 1. Effect of added butane on the conversion of **1** in the static gas-phase photolysis.

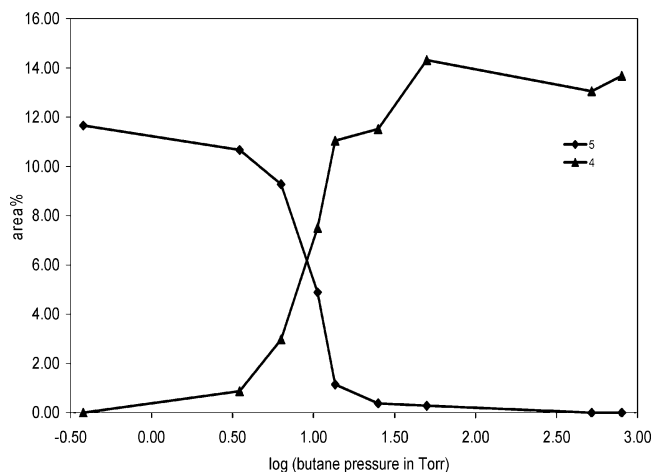


Figure 2. Effect of added butane on the formation of **4** and **5** in the static gas-phase photolysis of **1**.

Effect of Ar on the Gas-Phase Photochemistry of **1.** Argon was also used as a quencher gas in the photolysis of **1**. The product distribution, using 13 Torr of argon, is compared with that seen with the same pressure of butane in Table 2.

Time-Dependence Studies on the Gas-Phase Photochemistry of **1.** Time-dependence plots for the 254-nm light-initiated gas-phase photochemical reactions of **1** under static conditions with 13 Torr of butane are shown in Figures 4–6. The plots for the loss of starting material (Figure 4) and for the appearance of **2**, **3**, and the sum of **4** + **5** (Figure 5) all show good linearity (R^2 values of 0.997, 0.999, 0.998, and 0.995, respectively) with slopes of 0.96, 0.16, 0.16, and 0.42, respectively. There is an induction period for the formation of **6** (Figure 6).

Wavelength Effects on the Gas-Phase Photochemistry of **1.** The effect of excitation wavelength on the gas-phase photochemistry of **1** was studied under static conditions, both with and without butane present. Excitation with 254-nm light was achieved using a low-pressure mercury lamp, while 260, 266, and 270 nm excitation involved the use of lasers. The results are reported in Tables 1 and 2 in the Supporting Information section. The data for 254-nm irradiation are in terms of the relative amounts of the products, whereas an internal standard was used in the laser experiments. Thus, data for the latter are in absolute terms, and over 98% of the disappearance of **1** can be accounted for by the formation of the previously

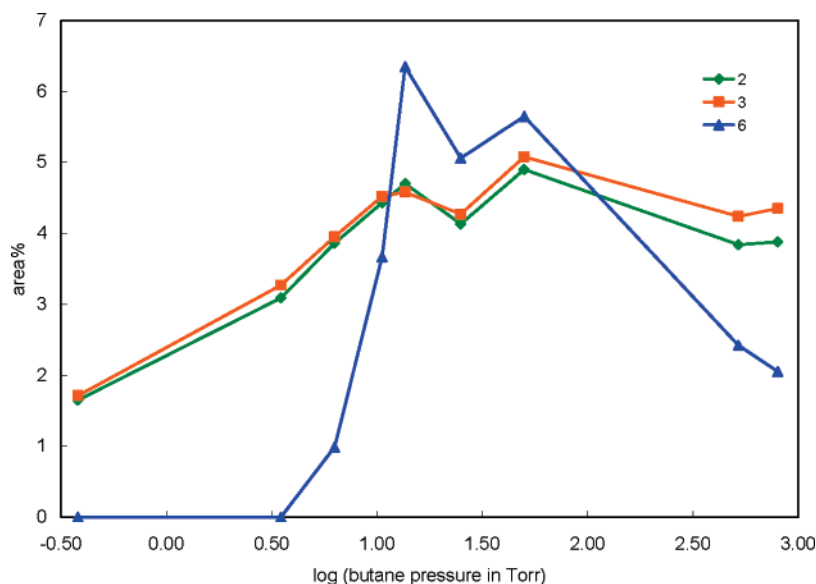


Figure 3. Effect of added butane on the formation of **2**, **3**, and **6** in the static gas-phase photolysis of **1**.

Table 2. Product Distributions from Photolysis of **1** with and without 13 Torr Butane or Argon^a

quencher	conversion %	2	3	4	5	6
none	21.0 ± 1.0	1.4 ± 0.1	1.4 ± 0.1	2.0 ± 0.1	11.6 ± 0.6	0.0
butane	29.0 ± 1.5	4.7 ± 0.1	4.6 ± 0.1	11.1 ± 0.3	1.1 ± 0.2	6.4 ± 0.3
Ar	30.0 ± 1.1	4.8 ± 0.1	4.6 ± 0.1	10.0 ± 0.4	2.2 ± 0.3	7.3 ± 0.5

^a Thirty-minute irradiation time; numbers represent area percents from GLC; Σ **2** – **6** \neq conversion because of minor products.

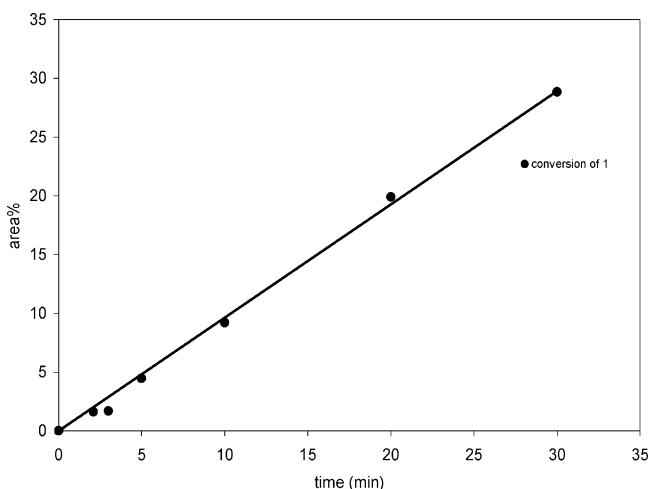


Figure 4. Time-dependence study for the loss of **1** upon photolysis with 13 Torr butane.

cited products in these photolyses. No wavelength effect on the product distribution was observed.

Photochemistry of Cycloadducts 2–4. The products **2–4** were isolated from preparative solution photolyses and individually photolyzed under flowing and static gas-phase conditions with 254-nm excitation. No photochemistry was observed in any of these photolyses.

Discussion

Photoproducts Formed in the Gas Phase in the Absence of a Quencher Gas. Only one photoproduct, compound **5**, is formed when **1** is photolyzed under flowing, that is, low-pressure (ca. 30 mTorr), conditions (see eq 2). The distribution of the

photoproducts formed in a typical “static” experiment at 300 mTorr of reactant is shown in Table 2. Here again **5** dominates, but the meta cycloaddition products, **2–4**, now also appear. Compounds **2–4** are the major products from photolysis in solution, as has been reported earlier^{3a} and confirmed in this work. Compound **5** was seen earlier as an artifact from the solution-phase photochemistry that appeared upon the insertion of **4** into a gas chromatograph at high temperature.^{3a}

Mechanistic Discussion Concerning the Formation of 5 in the Gas Phase. We rigorously confirmed that the formation of compound **5** was not due to thermal chemistry during our GLC analysis; we could readily lower the temperature of the injector and the column to a point where compound **4** was demonstrably stable and yet observe **5** as a photolysis product. We also have found compounds **2–4** to be photostable under flowing conditions, consistent with **5** being a primary photoproduct. However, it is obviously relevant that thermal excitation of **4** leads to **5**, through a mechanism that involves an unexceptional 1,5 hydrogen shift (see eq 3).^{3a}

The quencher gas experiments clearly indicate that vibrationally excited **4** is forming in the low-pressure gas-phase photolysis. The presence of butane or argon suppresses the formation of **5** and concomitantly increases the formation of **4** (see Figure 2 and Table 2). As one might expect, argon is modestly less effective as a collisional quencher than butane (Table 2). The overall conversion of **1** to photoproducts is significantly higher with a quencher gas present (see Figure 1 and Table 2). This will be discussed further below. The yield of **4** effectively plateaus when the butane pressure exceeds 50 Torr, and no **5** is observed at a butane pressure >500 Torr. Analysis of the data in Figure 2 indicates that the sum of **4** + **5** is relatively constant and minimally dependent on the butane pressure.

Though one could conceive that the S_1 state of **1** also needs to be vibrationally excited for “hot” **4** to be formed, there are good reasons to believe that this is not the case. The ground-state energies for compounds **1** and **4** were estimated by using electronic structure calculations at the B3LYP/6-31G**//B3LYP/3-21G* level of theory.¹⁷ These indicate that the ground-state

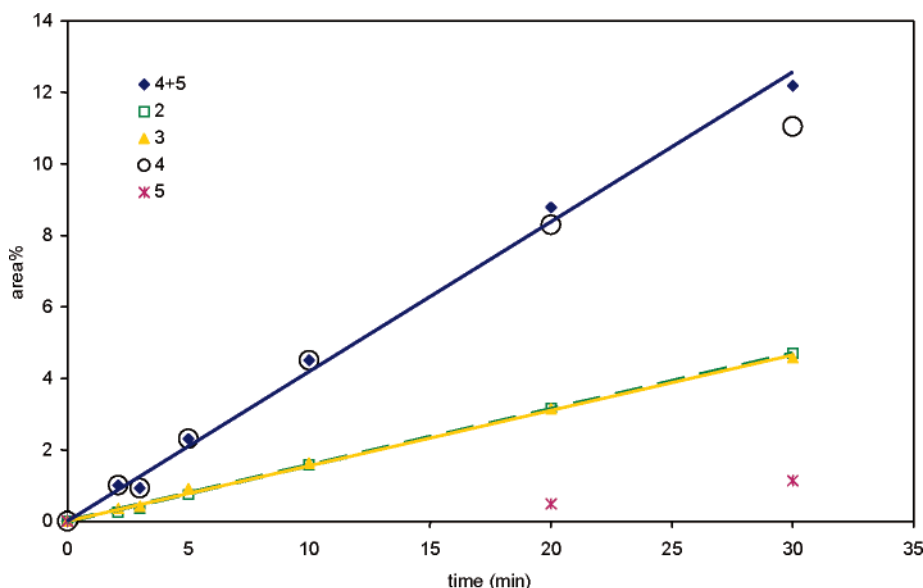


Figure 5. Time-dependence study for the formation of products **2–5** upon photolysis of **1** with 13 Torr butane. Though traces of **5** were detected by GLC at 5 and 10 min, the peaks were too small to be accurately integrated.

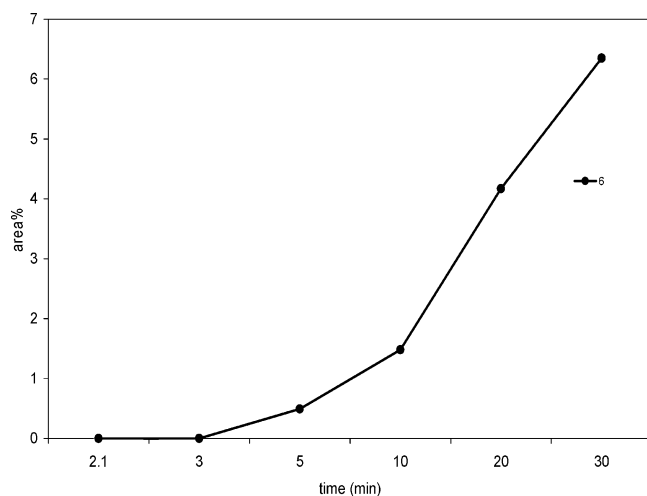
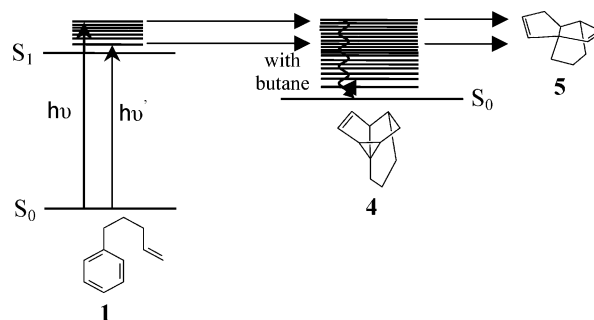


Figure 6. Time-dependence study for the formation of **6** upon photolysis of **1** with 13 Torr butane.

energy of **4** sits ca. 34 kcal/mol above that of **1**. By analogy with the spectroscopy of toluene vapor,¹⁸ we assign the 0,0 transition for **1** to ca. 267 nm (37500 cm⁻¹), which leads one to estimate that S₁[°] of **1** sits ca. 107 kcal/mol above the ground state. Thus, there could be as much as 73 kcal/mol of vibrational energy available to **4** upon its formation from S₁[°] of **1**. Since thermolysis at ca. 200 °C suffices to efficiently convert **4** to **5**, one can estimate the activation energy for this transformation to be ca. 30–35 kcal/mol. This is well below that which is available by electronic excitation of **1**.

Scheme 2. The Proposed Mechanism for the Formation of **5** in the Gas Phase



The results of the study of the effect of excitation wavelength on the photochemistry of **1**, under static conditions without quencher gas, also indicate that S₁^{vib} is not required to convert **4** to **5**. Excitation into the 0–0 transition of S₀ → S₁ (270 nm) gives a ratio of **4** to **5** that is comparable to that observed with 254-nm irradiation. Clearly, the conversion of **4** to **5** is not adversely affected by reducing the excess vibrational energy in the S₁ excited state of **1**.

We therefore propose the mechanism for the formation of **5** shown in Scheme 2. This mechanism correctly predicts that the ratio of **5** to **4** should diminish as quencher gas is added (ultimately going to zero in solution) but that the sum of **4** + **5** should be independent of quencher gas pressure.

Mechanistic Discussion Concerning the Formation of **2 and **3** in the Gas Phase.** It is clear that the reactions leading to the formation of these two meta cycloadducts are coupled, as has been noted earlier for the solution-phase studies (see Scheme 1). This is most evident in the time-course plot in Figure 5 where the two products show identical slopes. Interestingly, these two products are formed in essentially identical amounts in the gas phase (see Table 2 and Tables in the Supporting Information) but **3** is modestly favored over **2** in solution (Table 1).

These products differ from **4** in that they do not undergo thermolysis during gas chromatography. This may partly be a

(17) (a) Frisch, M. J.; Trucks, G. W.; Schlegel, H. B.; Scuseria, G. E.; Robb, M. A.; Cheeseman, J. R.; Zakrzewski, V. G.; Montgomery, J. A., Jr.; Stratmann, R. E.; Burant, J. C.; Dapprich, S.; Millam, J. M.; Daniels, A. D.; Kudin, K. N.; Strain, M. C.; Farkas, O.; Tomasi, J.; Barone, V.; Cossi, M.; Cammi, R.; Mennucci, B.; Pomelli, C.; Adamo, C.; Clifford, S.; Ochterski, J.; Petersson, G. A.; Ayala, P. Y.; Cui, Q.; Morokuma, K.; Malick, D. K.; Rabuck, A. D.; Raghavachari, K.; Foresman, J. B.; Cioslowski, J.; Ortiz, J. V.; Baboul, A. G.; Stefanov, B. B.; Liu, G.; Liashenko, A.; Piskorz, P.; Komaromi, I.; Gomperts, R.; Martin, R. L.; Fox, D. J.; Keith, T.; Al-Laham, M. A.; Peng, C. Y.; Nanayakkara, A.; Challacombe, M.; Gill, P. M. W.; Johnson, B.; Chen, W.; Wong, M. W.; Andres, J. L.; Gonzalez, C.; Head-Gordon, M.; Replogle, E. S.; Pople, J. A. *Gaussian 03*, Revision B.03; Gaussian, Inc.: Pittsburgh, PA, 1998. (b) We thank Professor Paul Wenthold for carrying out these calculations.

(18) (a) Ginsburg, N.; Robertson, W. W.; Matsen, F. A. *J. Chem. Phys.* **1946**, *14*, 511–517. (b) Burton, C. S.; Noyes, W. A., Jr. *J. Chem. Phys.* **1968**, *49*, 1705–1714.

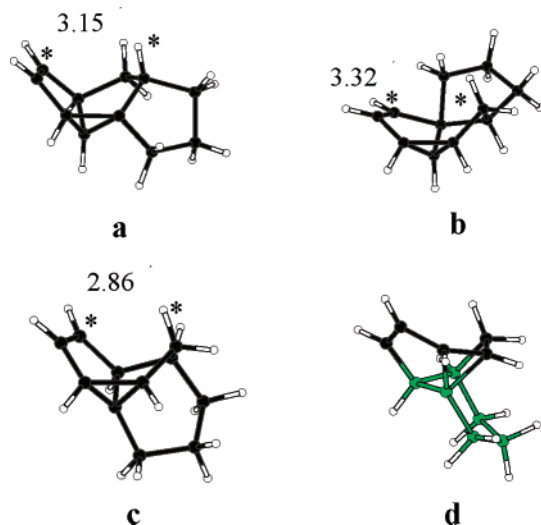


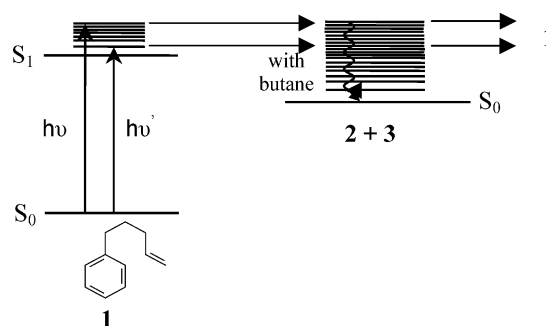
Figure 7. (a–c): Low-energy conformations for **2**, **3**, and **4** from MM⁺ calculations. (d) The low-energy conformation for **4** with the six-member ring highlighted.

consequence of their greater stability. The electronic structure calculations¹⁷ place the energies of **2** and **3** at 26 and 28 kcal/mol above that of **1**; recall that **4** is computed to lie 34 kcal/mol above **1**. Compound **4** is also better configured for the [1,5] hydrogen shift chemistry, as can be seen in the optimized structures shown in Figure 7a–c that were derived from MM⁺ molecular mechanics calculations. The distances between the key atoms, C* and H*, in **2**, **3**, and **4** are 3.15, 3.32, and 2.86 Å, respectively. The proximity of C* and H* in **4** is facilitated by the six-membered ring highlighted in Figure 7d that is unique to this adduct.

The formation of products **2** and **3** is modestly increased when a quencher gas is added (Figure 3). The effect is greater than for the sum of **4** + **5** (Table 2) and accounts for part of the increased conversion of **1** to photoproducts in the presence of quencher gas (Figure 1 and Table 2). The enhancement is maximized at a butane pressure of ca. 10 Torr (Figure 3). A study of the effect of excitation wavelength on product formation indicates that the yields of **2** and **3** are not improved by excitation with lower excess vibrational energy (table in Supporting Information). By the same argument as that used for the formation of **5**, this suggests that the excess vibrational energy in S₁^{vib} is unnecessary for the formation of **2** and **3**. This is consistent with their formation in the solution phase. However, the enhancement in their formation as a quencher gas is added indicates that either these products or some precursor species must be vibrationally cooled for **2** and **3** to be efficiently formed. There appears to be no chemical process that traps the hot product, since we see no set of related products akin to the **4/5** pair. The most logical alternative would be that the hot species returns to 5-phenyl-1-pentene. Employing Occam's Razor, we show "hot" **2** and **3** as the species returning to the starting material in Scheme 3 (however, see also further discussion below).

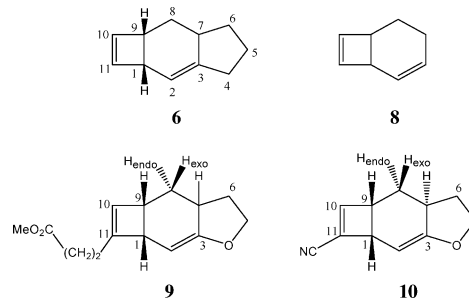
Compound 6. The most novel observation made during the butane-quenching studies was the appearance of a new product, **6**. By contrast with compounds **2**–**5**, there is no product reported in the solution-phase studies that would appear to correlate with this product. In fact, a reexamination of the solution-phase photochemistry showed that a trace amount of **6** is formed in solution with long photolysis times, and it was from such

Scheme 3. The Proposed Mechanism for the Formation of Cycloadducts **2** and **3** in the Gas Phase



irradiations that this material was eventually isolated. As shown in Figure 3, **6** is not observed at all in the absence of a quencher gas. Formation of **6** is optimized at ca. 13 Torr butane and then rapidly falls off as the quencher gas pressure is increased. In contrast with the linear time-course plots characteristic of the formation of **2**, **3**, and **4** + **5** (see Figure 5), the formation of **6** shows a pronounced induction period (Figure 6). It becomes a major product (exceeding **2** + **3**) with photolysis times longer than 10 min (for example, see Table 2). This induction period suggests that one or more transient intermediates are the source of **6**.

Structure Assignment of 6: an Ortho Photocycloaddition Product. GLC-mass spectral analysis showed the product to have a molecular ion at *m/e* = 146, isomeric with **1**. Its UV-vis absorption spectrum shows no absorption beyond 230 nm, an indication that the highly conjugated character of the benzene moiety in **1** has been destroyed. A comprehensive NMR spectral analysis clearly indicated that the structure of **6** is fundamentally different from the meta cycloadducts, and on the basis of the reasoning outlined below, we assign the structure of this compound to the ortho cycloadduct shown below. Also shown are three structures (**8**–**10**) that proved useful in interpreting the NMR spectra.



The NMR data available to us included ¹H and ¹³C NMR spectra as well as spectra from APT, ¹H–¹³C HMQC, and ¹H–¹H COSY experiments. The ¹H and ¹³C NMR spectra are shown in Figures 8 and 9, respectively. The ¹H chemical shifts of **6**, as well as chemical shift data for reference compounds **8**,^{19,20} **9**,²¹ and **10**,²² are summarized in Table 3. The *J* values for **6**, **9**, **10**, and cyclobutene are compiled in Table 4.^{21–23}

(19) Baldwin, J. E.; Kaplan, M. S. *J. Am. Chem. Soc.* **1971**, *93*, 3969–3977.
(20) Allred, E. L.; Beck, B. R.; Voorhees, K. J. *J. Org. Chem.* **1974**, *39*, 1426–1427.

(21) Vízvárdi, K.; Toppet, S.; Hoornaert, G. J.; Keukeleire, D. D.; Bakó, P.; Van der Eycken, E. *J. Photochem. Photobiol., A: Chem.* **2000**, *133*, 135–146.

(22) Al-Qaradawi S. Y.; Cosstick K. B.; Gilbert A. *J. Chem. Soc., Perkin Trans. I* **1992**, 1145–1148.

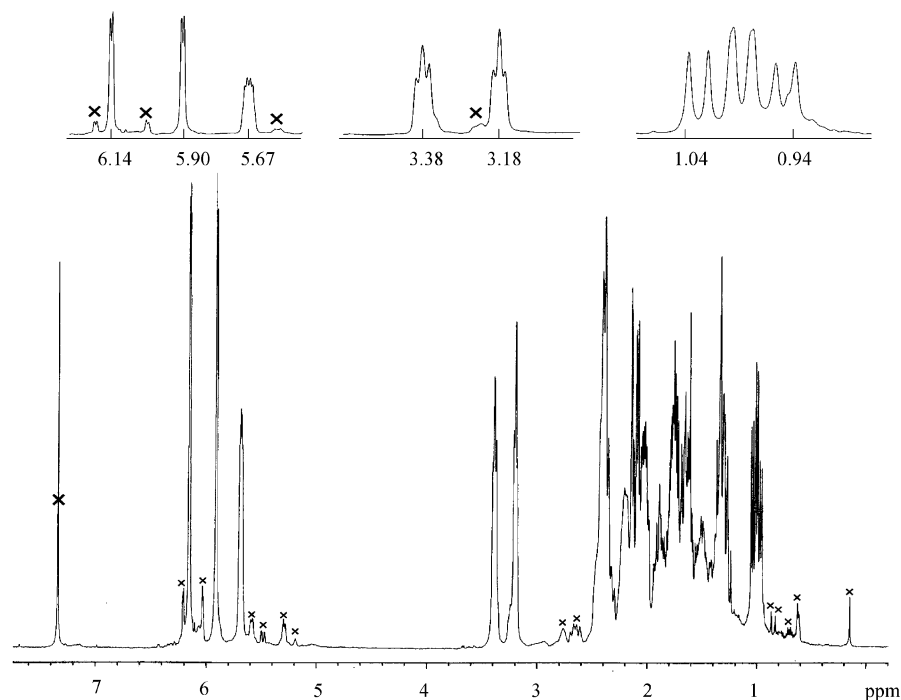


Figure 8. ^1H NMR spectrum of **6** in CDCl_3 ; peaks marked with \times are due to impurities.

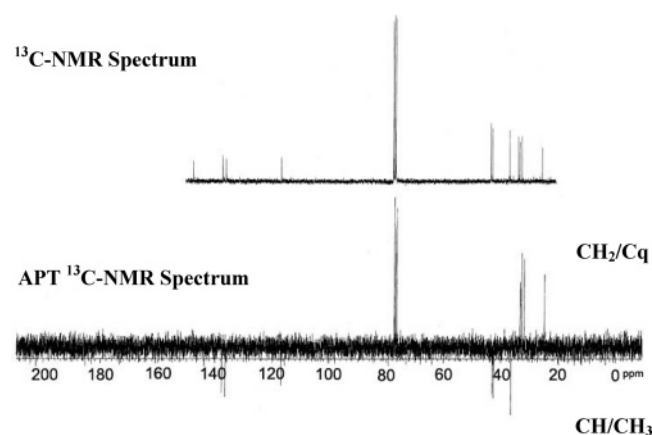


Figure 9. ^{13}C NMR and APT ^{13}C NMR spectra of **6** in CDCl_3 .

Table 3. ^1H NMR Data for **6**, **8**, **9**, and **10**

	6	8	9	10
δ_{H1}	3.38 (dd)	3.20–3.35 (br s)	2.92–3.02 (m)	3.2 (dd)
δ_{H2}	5.67 (dd)	5.70–5.90	4.87 (dd)	4.89 (dd)
δ_{H4}	2.33 (dd)			
δ_{H5}	1.40–1.70 (m)		4.17 (t) (exo)	4.89 (dds) (exo)
			3.92 (ddd) (endo)	3.50 (m) (endo)
δ_{H6}	1.14–1.39 (m)		1.65 (ddd) (exo)	1.5 (exo)
			2.00–2.50 (endo)	1.08 (m) (endo)
δ_{H7}	2.10–1.95 (m)	1.20–2.10	2.00–2.50	1.76 (m)
δ_{H8}	0.99 (m)	1.20–2.10	1.07 (ddd) (exo)	0.64 (m) (exo)
			2.00–2.50 (endo)	1.5 (endo)
δ_{H9}	3.18 (dd)	3.05–3.20 (br s)	3.20–3.30 (m)	2.56 (m)
δ_{H10}	5.90 (d)	5.70–5.90	5.64 (br s)	6.00 (d)
δ_{H11}	6.14 (d)	6.00–6.15 (d)		

The ^1H – ^{13}C HMQC and ^1H – ^1H COSY spectra (Supporting Information) provided the carbon connectivity. The assignment of the configuration between H1 and H9 is based on the coupling constant $J_{1,9}$. The consistency between the $J_{1,9}$ value in **6** and

Table 4. The J Values for the ^1H NMR Resonances of **6**, **9**, **10**, and Cyclobutene^a

	6	9	10	cyclobutene
$J_{1,2}$	5.7	6.3	5	
$J_{1,9}$	4.2		4	4.65
$J_{2,7}$	2.4 ^b	2.5	2.5	
$J_{10,11}$	2.4/2.7 ^c			2.85
J 's of H4	21.3, ^d 12.3			

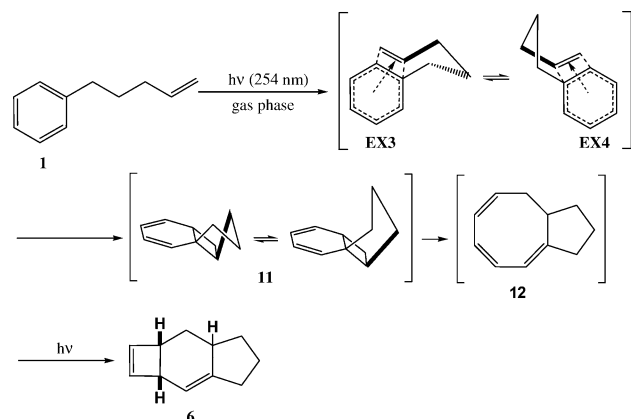
^a Coupling constants in Hz. ^b This coupling constant is obtained from the resonance in the ^1H NMR spectrum that corresponds only to H2. The peak corresponding to H7 is embedded in a multiplet that includes H7 plus one of the H6s. The $J_{2,7}$ could not be resolved from this peak. The assignment of this coupling constant is based on the reference values. ^c $J_{10,11}$ is 2.4 Hz in H11 and 2.7 Hz in H10. ^d This large J value may be due to the geminal coupling between the H4s. The $J_{6\text{gem}}$ in **10** is reported as 20 Hz.²²

those in reference compound **10** suggests a cis-H1,H9 configuration for **6**. This result is confirmed by a previous study of the coupling constants between the protons in cyclobutene,²³ which reported values of 4.65 Hz for J_{cis} and 1.75 Hz for J_{trans} between the vicinal methylene protons. The coupling constant between the vinyl protons in cyclobutene was also reported as 2.85 Hz in the same reference, which is consistent with our observation of 2.4 and 2.7 Hz from the ^1H NMR spectrum of **6**. In sum, the spectral data are consistent with the assignment of photoproduct **6** to the structure shown above.

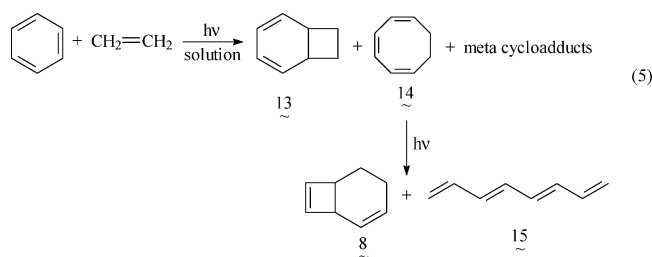
Mechanistic Discussion Concerning the Formation of **6 in the Gas Phase.** Considering the bonding present in **6**, the most logical origin for this compound is through intramolecular ortho cycloaddition of the alkene with the aromatic ring. Such [2+2] cycloaddition is a known photochemical reaction for certain, appropriately substituted, aryl alkenes.⁸ Two additional steps are necessary to generate **6** after the primary photoproduct is formed, but both are well-precedented.^{2e,8} The mechanism is shown in Scheme 4.

With regard to the initial cycloaddition reaction, intermolecular ortho photocycloaddition between benzene and ethene

(23) Hill, E. A.; Roberts, J. D. *J. Am. Chem. Soc.* **1967**, *89*, 2047–2049.

Scheme 4. Proposed Mechanism for the Formation of **6** in the Gas Phase

in solution has been reported (eq 5).²⁴ The primary cycloadduct, **13**, readily isomerizes in its ground state to its tautomer, cyclooctatriene (**14**). These are formed together with meta cycloadducts, which are, in fact, the major photoproducts. Only small amounts of **13** and **14** are present at high conversions; secondary photochemistry converts **14** to **8** and **15**.

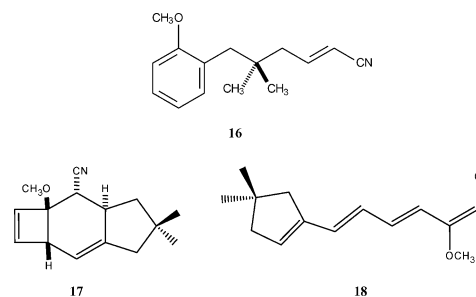


However, attempts to see intramolecular ortho cycloaddition with unsubstituted alkenyl benzenes in solution have generally been unsuccessful. Meta cycloaddition always dominates.^{2b,2d,8} One can achieve ortho cycloaddition by adding electron-donating and withdrawing substituents to the aryl and olefinic moieties, respectively, in substrates analogous to **1**.^{8,21,22,25,26} Success here is apparently due to the intervention of singlet exciplexes with appreciable charge-transfer character.^{25,27}

Exciplexes in which the olefin approaches the excited benzene in an exofacial manner are favored, since an endofacial approach would result in the formation of an excessively strained cycloadduct.²⁸ In Scheme 4, this leads to the exciplexes labeled as **EX3** and **EX4**, where the bolded bonds are those exo to the fused ring formed between the benzene ring and the olefin. Closure results in **11**, with the bolded bond now clearly occupying an exo-orientation. The subsequent steps mirror those proposed for the intermolecular system.

The primary cycloadducts are often labile and undergo facile thermal electrocyclic ring opening to bicyclo[6.3.0]undecatrienes.^{8,29} Secondary photochemistry then leads to disrotatory ring closure or electrocyclic ring opening. For example, irradiation of compound **16** gives **17** and **18** as the isolable products.²⁵ The analogy between compound **17** and our photoproduct, **6**, is evident; however, we have not observed a product equivalent to **18**.

(24) Mirbach, M. F.; Mirbach, M. J.; Saus, A. *Tetrahedron Lett.* **1977**, *11*, 959–962.



The pronounced induction period we observe for the formation of **6** (Figure 6) is consistent with the mechanism in Scheme 4. However, all attempts to detect intermediates **11** or **12**, by either GLC or by UV–vs absorption spectroscopy, have been unsuccessful. The precursors to **17** and **18** were likewise undetectable.²⁵

We are left with the question of why ortho cycloaddition of an unsubstituted phenylalkene such as **1** is readily observable in the gas-phase photolysis but minimally so in solution. We believe the quencher gas requirements for observing **6** provide some insight. This compound is unique among our products in that it is not observed at all in the absence of butane. It does resemble **5**, however, in that it is rapidly quenched by higher pressures of butane, in this case with pressures in excess of 100 Torr (Figure 3).³⁰ Collisional quenching ultimately reduces the formation of **6** to the point where it is found in only trace amounts, as in solution. As with the other products, the wavelength studies give no evidence of a wavelength effect on the formation of **6**. With these results in mind, and by analogy with our proposals to explain the effects of butane on the formation of the meta cycloadducts, one can extend the mechanism proposed in Scheme 4 to that shown in Scheme 5.

When the first intermediate, **11**, is formed with appreciable vibrational excitation, it may simply revert back to **1** in what is, in effect, a mode of radiationless decay. Compound **11** must be deactivated before it is stable enough to survive. However, some degree of vibrational excitation is required for **11** to ring-open to **12**; the optimal range is ca. 13 Torr of butane. In solution, or with high pressures of butane, **11** is quenched to the point where its conversion to **12** is minimal. Under either set of conditions, one might then anticipate detecting or isolating the cyclohexadiene, **11**, but as already noted, we have not yet been successful in doing so.

Alternatively, theoretical analyses of the ortho cycloaddition reaction suggest that this reaction is forbidden and that there is a barrier between the excited state of the reactants and the ultimate products.^{8,31,32} It is therefore plausible that the gas-

(25) Nuss, J. M.; Chinn, J. P.; Murphy, M. M. *J. Am. Chem. Soc.* **1995**, *117*, 6801–6802.

(26) Or by using carbonyl groups to induce intersystem crossing; see Wagner, P. J. *Acc. Chem. Res.* **201**, *34*, 1–8.

(27) See ref 8 for a critical discussion of the necessity for invoking an exciplex in the ortho cycloaddition mechanism.

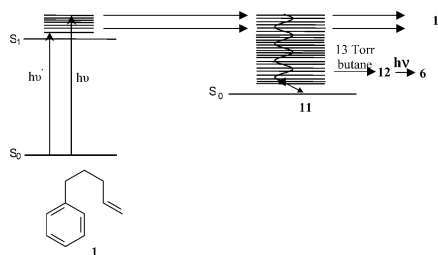
(28) Wender, P. A.; Siggel, L.; Nuss, J. M. *Org. Photochem.* **1989**, *10*, 357.

(29) Marvell, E. N. *Thermal Electrocyclic Reactions*; Academic Press: New York, 1980; p 260.

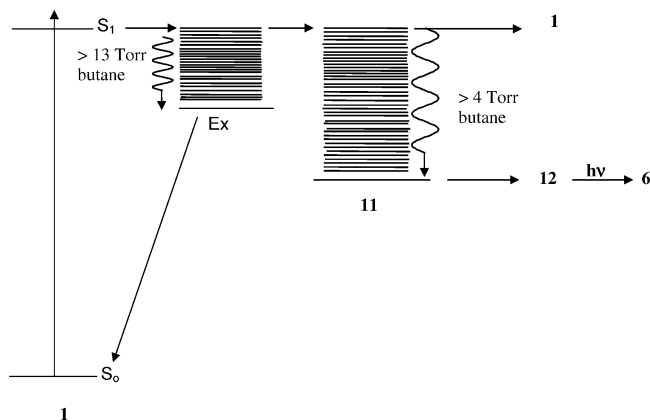
(30) This observation may explain why ortho cycloaddition was not observed in early studies of the intermolecular cycloaddition of photoexcited benzene to 2-butene. We estimate that that the pressures in these studies were at least 34-fold greater than the optimal (13 Torr) pressure for seeing ortho product. See: Kaplan, L.; Wilzbach, K. E. *J. Am. Chem. Soc.* **1968**, *90*, 3291–3292. Morikawa, A.; Brownstein, S.; Cvjetanovic, R. *J. Am. Chem. Soc.* **1970**, *92*, 1471–1476.

(31) Van der Hart, J. A.; Mulder, J. J. C.; Cornelisse, J. J. *Photochem. Photobiol., A: Chem.* **1995**, *86*, 141–148.

Scheme 5. A Possible Mechanism for Formation of **6** Taking into Account the Butane-Quenching Results



Scheme 6. An Alternative Mechanism for the Formation of **6**



phase reaction succeeds because the vibrational energy available to the reactants allows them to pass over this barrier. This would explain why the reaction is minimal in solution or with high pressures of butane but would not explain why the reaction is unobservable in the absence of butane. Reversion of “hot” **11** to **1** could explain the latter observation. This scenario is shown in Scheme 6.

Summary Mechanism. There continues to be debate about the exact description of the excited intermediates (exciplexes or otherwise) in these photochemical reactions.⁸ However, incorporating these species Schemes 3 and 4, and adding Scheme 6, we derive the summary mechanism shown in Scheme 7.

Conclusion

Photolysis of **1** in the gas phase produces meta cycloadducts common to the solution-phase photochemistry but also leads to products unique to the vapor phase. One such product, **5**, can be attributed to the initial formation of a meta cycloadduct (**4**) with excess vibrational energy. There is evidence that excess vibrational energy in two other meta cycloadducts (**2** and **3**) also lessens their formation. An intramolecular ortho cycloadduct (**6**) is also produced in the gas phase but only under a rather specific set of quencher gas pressures. This is the first time that intramolecular meta and ortho cycloaddition products have been seen simultaneously upon irradiation of a simple arylalkene hydrocarbon.

A mechanism for the formation of the cycloadducts is proposed (Scheme 7) on the basis of the results from buffer gas quenching and wavelength effect studies. In this mechanism, the alkene intercepts the excited aryl moiety to form a set of ortho and meta exciplexes, both in solution and in the gas phase.

However, the ortho exciplex cannot give a significant amount of ortho cycloadduct in the absence of vibrational excitation (as in solution) nor if the vibrational energy is too great (as in the gas phase in the absence of quencher gas).

It is interesting to speculate on the possibility of observing more extensive ortho cycloaddition in solution using fluorinated solvents that may less effectively deactivate the ortho exciplex species.

Experimental Section

The detailed experimental procedures for this work may be found in the doctoral dissertation of C. H. D. H.³³ The salient features are summarized below.

Instrumentation. Routine ¹H and ¹³C NMR spectra were obtained using Varian Gemini 200 MHz or Varian INOVA 300 MHz spectrometers. Chemical shifts are reported in deuteriochloroform in ppm relative to TMS or residual chloroform. Attached proton test (APT) and ¹H–¹H COSY spectra were acquired on a Varian INOVA 300 MHz Spectrometer. High resolution and ¹H–¹³C HMQC spectra were obtained on a Bruker DRX-500 (500 MHz) spectrometer. Mass spectra were recorded on a Finnigan 4000 mass spectrometer interfaced to a gas chromatograph containing either packed or capillary columns. Electron impact (EI) and chemical ionization (CI) mass spectra were recorded at 70 eV. Ultraviolet absorption spectra were collected in matched 1 cm² quartz cells using a Cary 100 spectrometer interfaced to a Pentium 100 MHz PC controlled by the Cary Scan Package software.

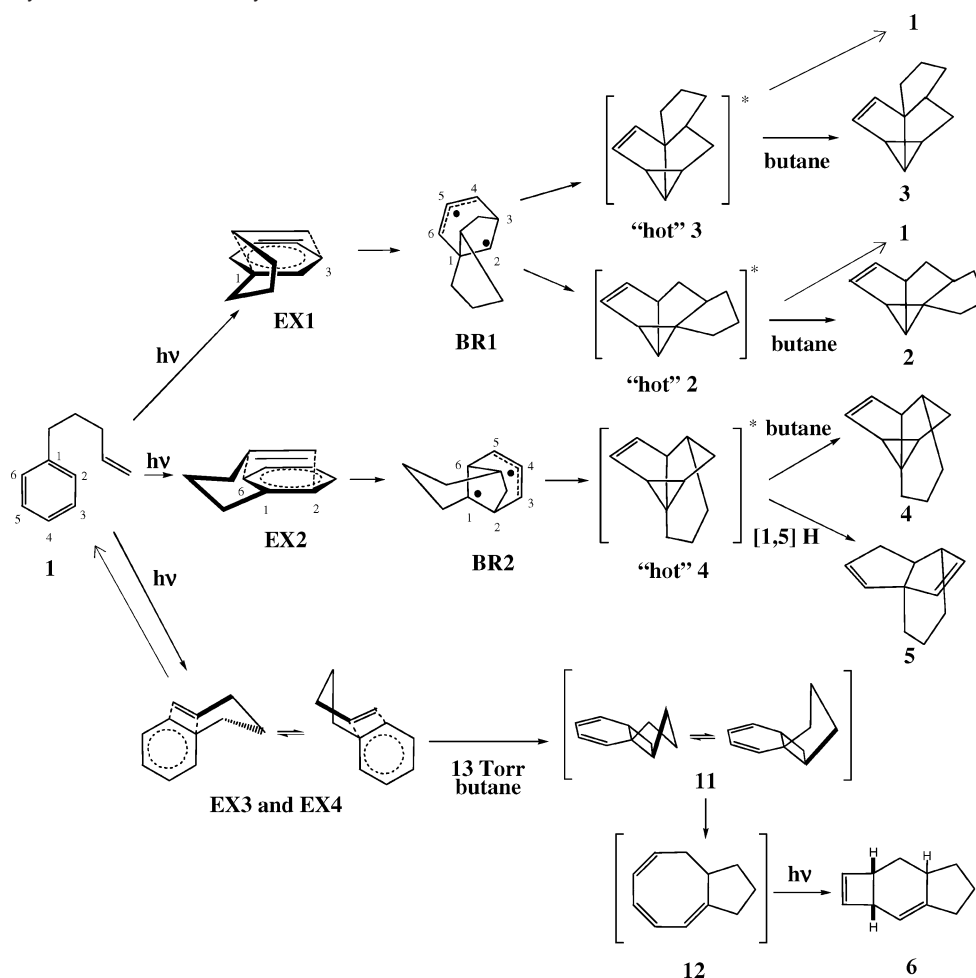
Analytical separations were performed on two capillary gas chromatographs: a Varian model Star 3400 CX and a Hewlett-Packard model 5890 series II. Both of the chromatographs were equipped with flame ionization detectors (FID). The chromatographs were integrated using either a Hewlett-Packard model 3390A or a model 3393A digital integrator. Preparative separations were performed using a Varian model 3300 TCD gas chromatograph equipped with a Hewlett-Packard model 3390A digital integrator. Columns used: A (J & W DB-1 30 m × 0.25 mm id., 0.25 μm), B (J & W Carbowax 30 m × 0.25 mm id., 0.25 μm), C (6 m × 0.25 in, 15% Carbowax 20M on 60/80 AW-DMCS Chromosorb W).

Computations. Molecular conformational optimizations were conducted on **2–4** using the MM+ force field found in HyperChem 6.03 (Hypercube). The steepest descent algorithm was used in all calculations. All geometries were optimized at the level with the root-mean-square gradient (RMS) of 0.1 kcal/mol. A maximum of 5000 cycles was set for each optimization if the calculation did not converge at the RMS level above. The ground-state energies for compounds **1–4** were estimated by using electronic structure calculations at the B3LYP/6-31G*/B3LYP/3-21G* level of theory. These calculations are reliable to ca. ±4 kcal/mol.

Solution-Phase Photochemistry. Experiments were done with matched quartz tubes (1-cm o.d.) in a Rayonet Model RPR-100 reactor (New England Ultraviolet Company) equipped with 16 254-nm low-pressure mercury lamps. All solution experiments were conducted in cyclohexane and degassed with argon for 30 min prior to photolysis. Quantum efficiencies at 255 and 266 nm were measured using a YAG-pumping dye laser (Continuum ND-60) operated with Coumarin 500 dye (Exciton Inc.) and a BBO (beta barium borate) doubling crystal. A 2× beam enlarger was used in front of the photolysis cell to avoid cell damage. The solutions were magnetically stirred during photolysis. The laser power passing through the sample cells was measured using an Ophir model AN/2 power meter. A power of 2–3 mW was used for the solution-phase photolyses.

(32) For a different view, see: Clifford, S.; Bearpark, M. J.; Bernardi, F.; Olivucci, M.; Robb, M. A.; Smith, B. R. *J. Am. Chem. Soc.* **1996**, *118*, 7353–7360.

(33) Ho, C.-D. D. Doctoral Dissertation, Purdue University, August, 2004.

Scheme 7. Summary Mechanism for Photolysis of **1** in the Gas Phase

Gas-Phase Photochemistry. The apparatus has been described in detail elsewhere.³⁴ Exploratory and preparative experiments were performed under flowing conditions. Briefly, a liquid sample was distilled (typically at pressures of 30 mTorr at 0 °C for **1**) through a quartz tube (33 cm in length \times 14.7 cm in circumference) surrounded by 16 254-nm low-pressure mercury lamps. The photolyzed vapor was collected in a liquid-nitrogen trap. After warming to room temperature, the trap was washed twice with 10 mL pentane, and the combined washings were concentrated under a stream of nitrogen. Exploratory experiments utilized 10–20 mg while preparative work employed 30–300 mg. The products were isolated by prep GLC equipped with column C.

Qualitative and quenching studies were performed under static conditions which involved filling a cylindrical quartz vessel (length 34 cm \times 4.7 cm o.d.) with the desired vapor to pressures of ca. 300 mTorr. The vessel was removed from the vacuum line and placed in a modified RPR-100 Rayonet reactor containing one 254-nm lamp for photolysis times of 30 min at 25 °C. Collection of the photolyzed sample required immersion of the vessel in liquid nitrogen and the injection of 5 mL pentane. After the vessel warmed to room temperature, the solution was removed and the vessel was again washed with pentane (5 mL). In the time-course study, the photolysis time was varied from 2 to 30 min in the presence of 13 Torr butane.

The samples were also photolyzed at different wavelengths using lasers. The laser power was always less than 13 mW to avoid two-photon excitation. The photolyses lasted from 20 min to 6 h depending on the laser power. The laser-photolyzed samples were washed with

pentane (5 mL) containing an internal standard. The combined pentane washings were concentrated under a stream of nitrogen and analyzed on columns A (80–100 °C) and B (90–110 °C). The gas-phase apparatus was designed with apertures to allow the introduction of a quencher gas (butane and Ar). Samples were degassed prior to flowing and static experiments by at least five freeze–pump–thaw cycles using 5 mTorr vacuum.

Solution Phase Photolysis of **1.** Solutions of 30–60 mM (0.5–1% w/v) **1** in cyclohexane were photolyzed at 254 nm for 20 min. Three products were identified as **2**, **3**, and **4** on the basis of the GLC retention times and by comparison of products to that reported in the literature.^{3b} Compound **6** was produced in a GLC detectable amount in photolyses longer than 60 min. Compounds **2–4** were isolated from preparative photolyses of **1** (60 mM, 114 mL) using AgNO₃-impregnated silica gel chromatography³⁵ followed by preparative GLC. Compound **6** was isolated using AgNO₃-impregnated silica gel chromatography. The ¹H NMR spectral data of **2–4** are consistent with those published in the literature.^{3a}

Photolysis of **1 in the Gas Phase under Flowing Conditions.** A 24-mg sample of **1** was photolyzed in the gas phase under flowing conditions with 254-nm light. The sample was kept at 0 °C, resulting in a pressure of 30 mTorr. Compound **5** was isolated by preparative GLC and found to have ¹H NMR spectral data consistent with the those published.^{3a}

Photolysis of **1 in the Gas Phase under Static Conditions.** A static photolysis cell with 300 mTorr of **1** was prepared. The sample was kept at 0 °C to provide the proper vapor pressure for photolysis. The

(34) Suarez, M. L.; Duguid, R. J.; Morrison, H. J. *Am. Chem. Soc.* **1989**, *111*, 6384–6391.

(35) Li, T. S.; Li, J. T.; Li, H. Z. *J. Chromatogr., A* **1995**, *715*, 372–375.

isolated product mixture in pentane was concentrated and analyzed by GLC. Each product was identified by GLC retention time, GLC co-injection with the product isolated from preparative solution phase photolysis, and GLC-mass spectrometry.

Acknowledgment. We thank Professor Paul Wenthold for carrying out the electronic structure calculations and for helpful discussions.

Supporting Information Available: ^1H - ^{13}C HMQC and ^1H - ^1H COSY NMR spectra for compound **6**. Tables (1 and 2) showing the effect of excitation wavelength on product distribution. The UV absorption spectrum of **1** in cyclohexane. This material is available free of charge via the Internet at <http://pubs.acs.org>.

JA044504Z